A HMSIW Circularly Polarized Leaky-Wave Antenna With Backward, Broadside, and Forward Radiation

Ali Pourghorban Saghati, *Student Member, IEEE*, Mir Mojtaba Mirsalehi, and Mohammad Hassan Neshati, *Senior Member, IEEE*

***Abstract*—A miniaturized frequency-scanning leaky-wave antenna (LWA) with circular polarization (CP) and backward-broadside-forward radiation is presented. Half-mode substrate integrated waveguide (HMSIW) in combination with interdigital capacitors (IDCs) is utilized in order to achieve a composite right/left-handed leaky-wave structure. Ramp-shaped slots are introduced as interdigital capacitors. Using this structure, the balanced condition (in which series and shunt resonances are equal) can be obtained for the unit-cell. As a result, wide bandwidth of 7.4–13.5 GHz with continuous angular scanning of $\sim -70^\circ$ to 70° is achieved. The axial ratio in the direction of the main beam is lower than 3.1. The performance of the antenna is measured, and close agreement between the simulation and measurement is observed.**

***Index Terms*—Composite right/left-handed (CRLH), half-mode substrate integrated waveguide, leaky-wave antennas, metamaterials.**

I. Introduction

HALF-MODE substrate integrated waveguides (HMSIWs) have become popular in the design of leaky-wave antennas (LWAs) over the past years. They have all the advantages of SIW structures, while approximately reducing the size by half [1]. Various frequency-scanning SIW/HMSIW LWAs have been presented so far [2]–[6]. However, despite their advantages, continuous backward to forward scanning, including the broadside radiation, is not achieved for the proposed structures. A remedy to this issue is introduced in [7] and [8], where composite right/left-handed (CRLH) SIW transmission lines (TLs) are used in the LWA implementation. By using these CRLH structures, in addition to conventional right-handed frequency region (parallel phase and group velocity), wave propagation in left-handed frequency region (anti-parallel phase and group velocity) is also observed. This occurs due to the simultaneous negative permittivity (ε) and permeability (μ) in this region [9], [10]. Therefore, negative radiating wavenumber results in backward radiation. However, at the transition point, where the radiating wavenumber becomes zero, the broadside radiation can be achieved.

Manuscript received January 11, 2014; revised February 11, 2014; accepted February 25, 2014. Date of publication March 04, 2014; date of current version March 18, 2014.

The authors are with the Electrical Engineering Department, Ferdowsi University of Mashhad, Mashhad 9177948974, Iran (e-mail: ali.pourghorban@stu.um.ac.ir; mirsalehi@um.ac.ir; neshat@um.ac.ir).

Color versions of one or more of the figures in this letter are available online at http://ieeexplore.ieee.org.

Digital Object Identifier 10.1109/LAWP.2014.2309557

On the other hand, HMSIW structures can act as a host medium for CRLH TL, as the via-wall can be considered as an effective shunt inductor. Therefore, only series capacitors are needed to have an engineered CRLH TL. The use of interdigital capacitors (IDCs) with the HMSIW structure has been investigated in [7] and [11] to achieve CRLH-based LWAs. In [7], miniaturized frequency-scanning linearly polarized (LP) HMSIW LWAs are presented. However, the broadside radiation is not achieved as a result of no balanced condition for the proposed unit cells. In [11], a fixed-frequency electronically beam-steerable LWA, using CRLH HMSIW structure, is proposed. Series and shunt varactor diodes are used in order to achieve dynamic full-space scanning. In [12]–[14], embedded patches are also used in order to produce the series capacitance needed to have CRLH SIW/HMSIW structures. However, this method suffers from complexities in fabrication process due to the employed multilayered structure.

In this letter, a miniaturized frequency-scanning HMSIW LWA with circular polarization (CP) and backward-broadside-forward radiation is proposed. The ramp-shaped slots are introduced as series IDCs. The proposed structure consists of 16 unit cells and acts as a CRLH-based LWA, as will be shown. The beam scanning of $\sim -70^\circ$ to 70° over the frequency range of 7.4–13.5 GHz is achieved for the proposed antenna. Also, the antenna benefits from easy fabrication process of one-layer structure. To the best of the authors' knowledge, this is the first presentation of a circularly polarized HMSIW LWA with frequency-scanning beam-steering capability, covering both first and second quadrants.

II. Antenna Structure and Design

Fig. 1(a) and (b) shows the 3-D and top views of the proposed HMSIW unit cell. The top and bottom walls of the HMSIW structure can equivalently be modeled as series inductance and shunt capacitance, both distributed along the structure [7]. The ramp-shaped slots act as series IDCs, which along with the distributed shunt inductance due to sidewall vias, guarantee the wave propagation in the left-handed region. In order to achieve backward-to-forward scanning, including broadside radiation, balanced condition must be satisfied for the proposed unit cell, which means there has to be no band-gap between the left- and right-handed regions [7]. As can be seen in Fig. 1, some of the vias are removed in the HMSIW structure, where the IDCs are etched on the top metal. As a result, the value of the effective shunt inductance is reduced. The leakage from these gaps is negligible and, thus, has no significant effect on the LWA's guiding and radiation performance. This also has been

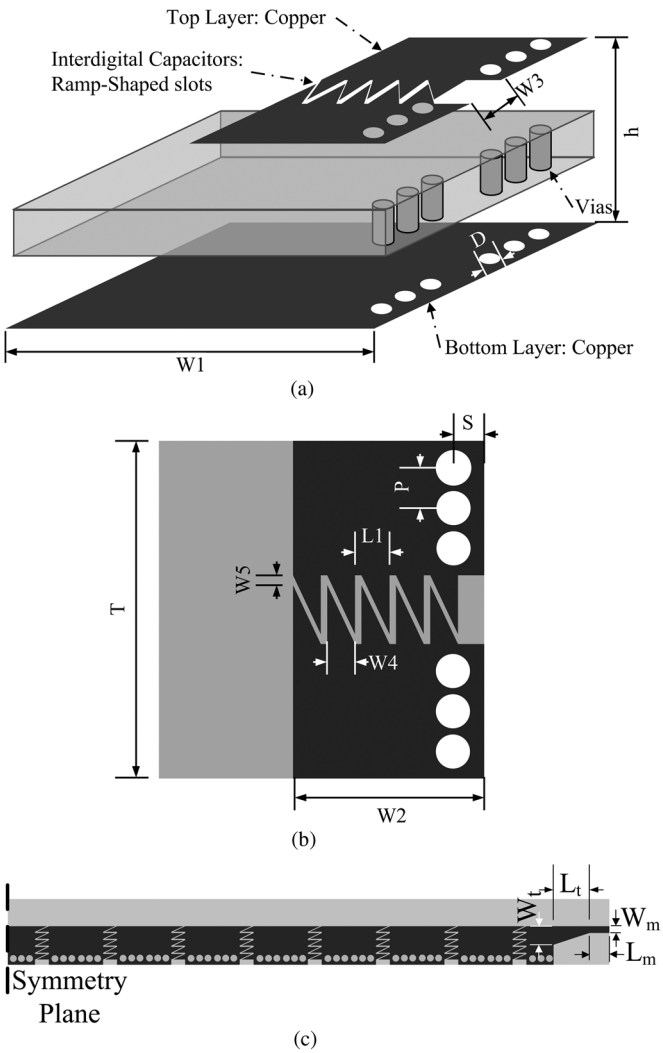

Fig. 1. (a) 3-D view of the proposed CRLH HMSIW unit cell structure. (b) Top view of the proposed unit cell structure. The parameter values are: $W_1 = 12$ mm, $W_2 = 6$ mm, $W_3 = 2.5$ mm, $W_4 = 0.85$ mm, $W_5 = 0.5$ mm, $h = 0.76$ mm, $L_1 = 1.1$ mm, $S = 1.2$ mm, $P = 1.2$ mm, $T = 10$ mm, $D = 1$ mm. (c) Top view of the symmetrical half of the presented CRLH HMSIW LWA. The parameter values are: $W_t = 2.9$ mm, $W_m = 1.16$ mm, $L_t = 4.5$ mm, $L_m = 3$ mm.

verified by simulation results using High Frequency Structure Simulator (HFSS). Also, each section is coupled capacitively to the next one using the IDCs, which makes the control of the left-handed frequency band simpler. With a defined cutoff frequency, the balanced condition can be achieved for the unit cell by adjusting the values of W_3, W_4, and W_5 (IDC parameters). Changing these three parameters only affects the left-handed region. However, the right-handed region remains almost the same. Consequently, equal shunt and series resonances can be achieved for the proposed unit cell, and thus the band-gap between these two regions is closed. Therefore, the values of both the effective shunt inductance and series capacitance are responsible in obtaining the balanced condition. The final dimensions of the presented unit cell are mentioned in the caption of Fig. 1.

In order to better study the behavior of the presented structure, the dispersion curve of a single cell is used [15]. There are two ways to extract the dispersion curve of the unit cell: 1) eigen-mode simulation using periodic boundary conditions, and 2) S-parameters extracted using driven-mode simulations [7]. While the former is more accurate, the latter is less time-consuming. In this letter, the second method is applied to the CRLH HMSIW unit cell illustrated in Fig. 1 using HFSS. Wave-port excitation at both ends of the unit cell is used, and the S-parameters of the unit cell are extracted. Then, the dispersion curve is retrieved, using the simulated S-parameters [15]. The antenna simulations and, later on, the measurement results verify that the dispersion curve results achieved using this method are correct. Fig. 2 shows the extracted dispersion curve. As can be seen, the transition between the right- and left-handed regions occurs at ~9 GHz. Therefore, using the ramp-shaped interdigital slots, seamless transition from left-handed to right-handed region (balanced condition) is achieved.

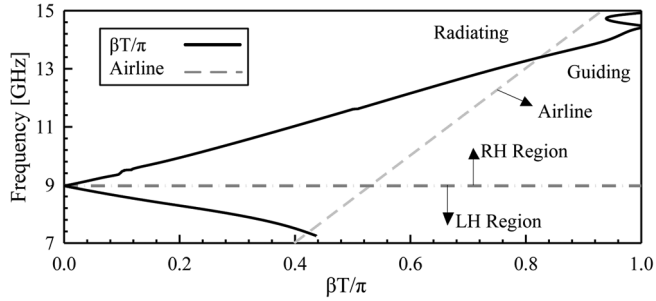

Fig. 2. Dispersion curve of the CRLH HMSIW unit cell shown in Fig. 1.

Fig. 1(c) shows the top view of the designed LWA. Sixteen unit cells of Fig. 1(b) are connected to each other in series, and taper-line transitions at input and output ends are used in order to match the structure to the 50-Ω microstrip lines. Parameters W_t and L_t are sized to provide matching to 50 Ω. As the wave is propagating from the input port to the output port, the power leaks out from both the ramp-shaped slots on the top metal layer and the open side of the HMSIW structure. As a result, the value of the height-to-width ratio (HWR) of the HMSIW must be chosen properly in order to produce the desired leakage radiation from the open side of the HMSIW structure. As was inspected during the design procedure, larger values for the HWR result in higher back-lobe levels in E-plane and lower values for the HWR reduce the leakage from the open side of the HMSIW structure. The width of the HMSIW top layer is among the parameters that are determined by the desired cutoff frequency. The value of the substrate thickness is chosen to be 0.76 mm in order to produce the desired leakage radiation from the open side. Moreover, the width of the bottom layer is chosen to be 2 times the width of the HMSIW top layer in order to minimize back-lobe levels, and therefore improve the radiation gain of the antenna. Because of radiation from both the ID slots and the HMSIW open wall, radiated electric fields with nearly equal magnitudes and phases with a difference of ~90° can be achieved [11]. This means that in comparison to the structures introduced in [7] with LP radiation, possibly the radiation from the designed antenna is circularly polarized. The simulated surface current distribution on the top layer of the proposed HMSIW unit cell at 12 GHz is shown in Fig. 3. The

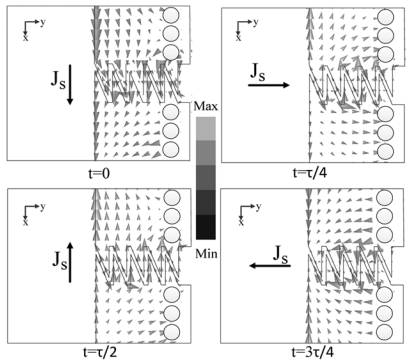

Fig. 3. Simulated surface current distributions on the proposed HMSIW unit cell.

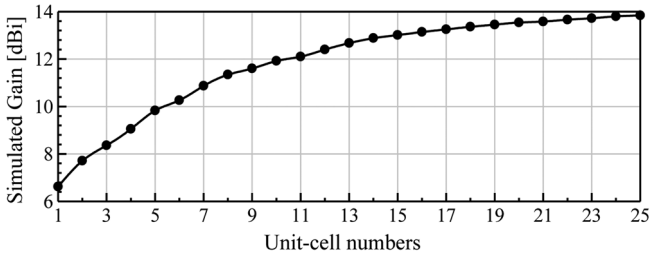

Fig. 4. Simulated antenna gain with different unit-cell numbers at 10.5 GHz.

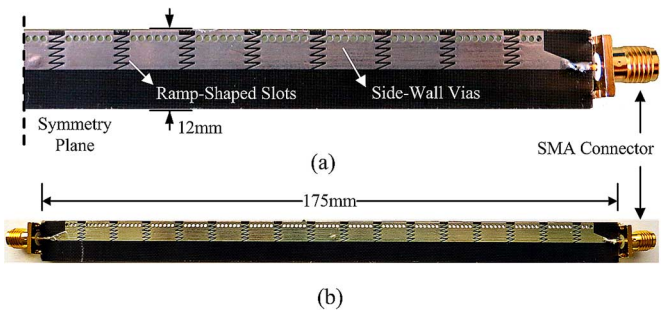

Fig. 5. (a) Symmetrical half of the fabricated HMSIW LWA. (b) Top view of the fabricated HMSIW LWA.

dominant surface current direction is depicted in each section. As can be seen, the current rotates counterclockwise, which implies right-handed CP (RHCP) [16].

Fig. 4 shows the antenna gain with respect to the number of the proposed unit cells at 10.5 GHz. As can be seen, the antenna gain is increased up to the case for the LWA with 17 unit cells. After that point, the gain is almost saturated. As a result, the case with 16 unit cells has been chosen for the proposed antenna.

Consequently, using the ramp-shaped slots along with the HMSIW structure brings the advantage of having both wideband frequency response and the circular polarization, which can be very useful in the space scanning applications. Also, due to the satisfied balanced condition, achieving broadside radiation is made feasible.

III. Experimental Results

The HMSIW LWA is fabricated on a 0.76-mm-thick Taconic TLY substrate using printed circuit board (PCB) technology.

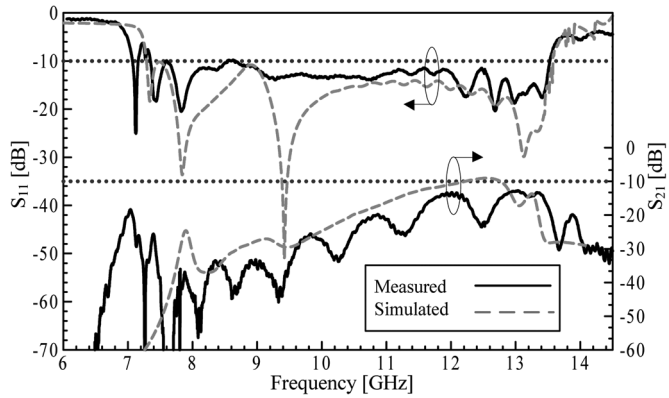

Fig. 6. Simulated and measured S_{11} and S_{21} for the proposed HMSIW LWA.

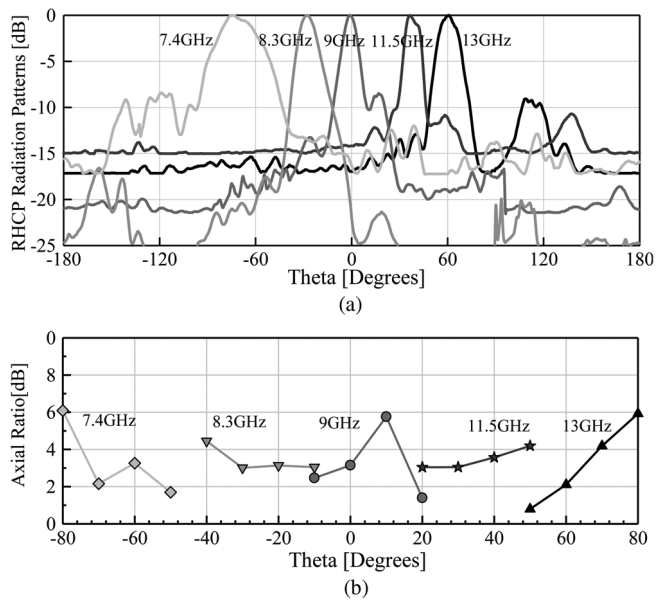

Fig. 7. (a) Measured RHCP E-plane radiation patterns. (b) Measured axial ratios for 7.4, 8.3, 9, 11.5, and 13 GHz.

TABLE I
Antenna Gain in the Direction of the Main Beam

Freq. (GHz)	Meas. (dBi)	Simu. (dBi)	Freq. (GHz)	Meas. (dBi)	Simu. (dBi)
7.4	7.48	8.94	10.3	10.04	13.14
8.3	9.20	11.3	11.5	11.49	14.3
8.7	8.93	11.34	12.6	11.72	14.48
9	8.65	12.05	13	12.01	14.56

The fabricated antenna is shown in Fig. 5. In order for the details to be visible, the symmetrical half of the fabricated antenna is depicted in Fig. 5(a). Simulated and measured S_{11} and S_{21} are depicted in Fig. 6, and good agreement is observed. The reflection coefficient, in the 7.4–13.5-GHz range, is lower than -10 dB. The measured insertion loss, in the same range, is higher than 13 dB, and the seamless transition between the left- and right-handed regions occurs at $\sim$9 GHz.

Fig. 7(a) shows the measured RHCP E-plane radiation patterns at different frequencies. The measured axial ratio versus theta is depicted in Fig. 7(b). The axial ratio lower than 3.1 in the direction of the main beam is observed for the fabricated

TABLE II
COMPARISON OF MINIATURIZED HMSIW LWAS

Structure	Antenna Type	Scanning Type	Backward & forward beam scanning / broadside radiation	Pol.	Bandwidth (GHz)	Gain (dBi)
[7]	HMSIW/ Modified HMSIW with IDCs	Freq. Scanning	Yes / No	LP	~8.5-9.4&10.5-13/ ~8.7-9.6&10-13	~7.8-10.6/ ~9.6-11.6
[11]	HMSIW with IDCs & Varactor Diodes	Fixed Freq. Electronically beam-steerable	Yes / Yes	CP	N/A	~7.8-11.30
[12]	HMSIW with embedded patches (Multilayered)	Fixed Freq. Electronically beam-steerable	Yes / Yes	LP	N/A	~11-14 (Simulated Gain)
This Work	**HMSIW with ramp-shaped IDCs**	**Freq. Scanning**	**Yes / Yes**	**CP**	**~7.4-13.5**	**~7.48-12.01**

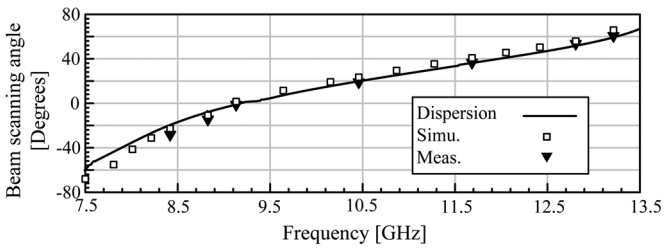

Fig. 8. Beam-scanning angle extracted from dispersion curve, electromagnetic (EM) simulation, and measurement results.

antenna, which verifies the CP radiation. As was expected, the cross polarization corresponds to LHCP, as the radiation level for the LHCP pattern is much lower (~ -15 dB) than the RHCP one. The measured and simulated gains of the proposed HMSIW LWA at different frequencies are tabulated in Table I. Differences in measured and simulated antenna gains would probably correspond to the effect of practical losses such as the connectors' losses and imperfect load termination, which are not considered in simulations.

Fig. 8 demonstrates the beam-scanning angle as a function of frequency, extracted from dispersion curve, simulation, and measurement. A continuous beam scanning of about $-70°$ to $70°$ in the interested frequency band (7.5–13.5 GHz) is achieved. The performance parameters of the implemented antenna are compared to relevant works in literature in Table II. The proposed antenna is capable of radiation in the broadside direction with CP. As can be seen in Table II, significant bandwidth improvement (as a result of the balanced condition) is achieved compared to [7]. Also, continuous frequency scanning is achieved, which has the advantage of no need to lossy components such as p-i-n or varactor diodes as well as biasing circuits over the ones that use the varactor based beam steering technique in [11] and [12].

IV. CONCLUSION

A frequency-scanning HMSIW LWA with CP radiation is presented. Ramp-shaped slots are introduced as IDCs. Matched balanced condition is obtained for the unit cell. As a result, continuous angular scanning of $\sim -70°$ to $70°$, over the wide bandwidth of 7.4–13.5 GHz is observed. A measured antenna gain of about 7.8–12 dBi is achieved. Also, significant reduction in size, due to use of CRLH metamaterial structures, is achieved. Therefore, this structure can be considered as a useful one in practical broadband applications.

REFERENCES

[1] W. Hong, B. Liu, Y. Wang, Q. Lai, H. Tang, X. X. Yin, Y. D. Dong, Y. Zhang, and K. Wu, "Half mode substrate integrated waveguide: A new guided wave structure for microwave and millimeter wave application," in *Proc. Joint 31st Int. Conf. Infr. Millim. Waves*, Sep. 18–22, 2006, pp. 219–219.

[2] J. Xu, W. Hong, H. Tang, Z. Kuai, and K. Wu, "Half-mode substrate integrated waveguide (HMSIW) leaky-wave antenna for millimeter-wave applications," *IEEE Antennas Wireless Propag. Lett.*, vol. 7, pp. 85–88, 2008.

[3] Y. J. Cheng, W. Hong, and K. Wu, "Millimeter-wave half mode substrate integrated waveguide frequency scanning antenna with quadri-polarization," *IEEE Trans. Antennas Propag.*, vol. 58, no. 6, pp. 1848–1855, Jun. 2010.

[4] Q. Lai, C. Fumeaux, and W. Hong, "Periodic leaky-wave antennas fed by a modified half-mode substrate integrated waveguide," *Microw., Antennas Propag.*, vol. 6, no. 5, pp. 594–601, Apr. 2012.

[5] J. Liu, D. R. Jackson, and Y. Long, "Substrate integrated waveguide (SIW) leaky-wave antenna with transverse slots," *IEEE Trans. Antennas Propag.*, vol. 60, no. 1, pp. 20–29, Jan. 2012.

[6] Y. J. Cheng, W. Hong, K. Wu, and Y. Fan, "Millimeter-wave substrate integrated waveguide long slot leaky-wave antennas and two-dimensional multibeam applications," *IEEE Trans. Antennas Propag.*, vol. 59, no. 1, pp. 40–47, Jan. 2011.

[7] Y. Dong and T. Itoh, "Composite right/left-handed substrate integrated waveguide and half mode substrate integrated waveguide leaky-wave structures," *IEEE Trans. Antennas Propag.*, vol. 59, no. 3, pp. 767–775, Mar. 2011.

[8] Y. Mizumori, K. Okubo, M. Kishihara, J. Yamakita, and I. Ohta, "Backfire-to-endfire radiation characteristics of CRLH-TL using substrate integrated waveguide and metal-patches," in *Proc. Asia-Pacific Microw. Conf.*, Dec. 7–10, 2009, pp. 1419–1422.

[9] C. Caloz, T. Itoh, and A. Rennings, "CRLH traveling-wave and resonant metamaterial antennas," *IEEE Antennas Propag. Mag.*, vol. 50, no. 5, pp. 25–39, Oct. 2008.

[10] A. Sanada, C. Caloz, and T. Itoh, "Characteristics of the composite right/left-handed transmission lines," *IEEE Microw. Wireless Compon. Lett.*, vol. 14, no. 2, pp. 68–70, Feb. 2004.

[11] A. Suntives and S. V. Hum, "A fixed-frequency beam-steerable half-mode substrate integrated waveguide leaky-wave antenna," *IEEE Trans. Antennas Propag.*, vol. 60, no. 5, pp. 2540–2544, May 2012.

[12] A. Suntives and S. V. Hum, "An electronically tunable half-mode substrate integrated waveguide leaky-wave antenna," in *Proc. Eur. Conf. Antennas Propag.*, Rome, Italy, Apr. 11–15, 2011, pp. 3828–3832.

[13] Nasimuddin, Z. N. Chen, and X. Qing, "Multilayered composite right/left-Handed leaky-wave antenna with consistent gain," *IEEE Trans. Antennas Propag.*, vol. 60, no. 11, pp. 5056–5062, Nov. 2012.

[14] Nasimuddin, Z. N. Chen, and X. Qing, "Substrate integrated metamaterial-based leaky-wave antenna with improved boresight radiation bandwidth," *IEEE Trans. Antennas Propag.*, vol. 61, no. 7, pp. 3451–3457, Jul. 2013.

[15] D. R. Smith, D. C. Vier, T. Koschny, and C. M. Soukoulis, "Electromagnetic parameter retrieval from inhomogeneous metamaterials," *Phys. Rev. E*, vol. 71, no. 3, pp. 036617(1)–036617(11), 2005.

[16] K. G. Thomas and G. Praveen, "A novel wideband circularly polarized printed antenna," *IEEE Trans. Antennas Propag.*, vol. 60, no. 12, pp. 5564–5570, Dec. 2012.